Mechanics & Industry **25**, 2 (2024)

https://doi.org/10.1051/meca/2023043

Mechanics & Industry

Available online at:
www.mechanics-industry.org

REGULAR ARTICLE

OPEN ACCESS

Pre-matching study of the natural gas engine turbocharging system based on the coupling of experiments and numerical simulation

Feng Zhou[1,2], Zichao Meng[1], Xu Xiao[2], Jianqin Fu[3], Kainan Yuan[2,*], Zhuangping Cui[2], Juan Yu[1], and Jingping Liu[3]

[1] College of Mechanical and Electrical Engineering, Central South University of Forestry and Technology, Changsha 410004, PR China
[2] China Machinery International Engineering Design and Research Institute Co., Ltd., Changsha 410000, PR China
[3] State Key Laboratory of Advanced Design and Manufacturing for Vehicle Body, Hunan University, Changsha 410082, PR China

Received: 18 August 2023 / Accepted: 24 November 2023

Abstract. In this study, a pre-matching method was developed based on measured performance parameters and theoretical calculations of turbochargers. First, the turbocharger of a natural gas engine was subjected to a comprehensive performance experiment. According to the experimental results, the maximum efficiencies of the turbine and compressor are 70% and 75%, respectively, and the efficiency of the turbine drops sharply from 70% to 56.6% as the pressure ratio increases from 1.25 to 2.4. In this thesis, a specific turbocharger pre-matching software has been developed in conjunction with a database. Three turbines and three compressors were selected from the self-developed database for matching and comparative study using this method. The simulation results showed that the maximum efficiency of turbine #1, #2 and #3 is 71.3%, 72.2% and 72.7%, respectively, and the efficiency of these three turbines is concentrated between 65% and 72.5%. Obviously, the maximum efficiency of the turbine has increased by 1.3–2.7% and the overall efficiency has improved after the pre-matching. Therefore, this developed pre-matching method can reduce time cost, improve work efficiency and engine performance, and is important for the design and development of turbochargers.

Keywords: Turbocharger / natural gas engine / pre-matching / numerical development technology

1 Introduction

Conventional fuels, as non-renewable resources, are mixtures of hydrocarbon derivatives, including coal, fuel oil and gas [1]. Due to the over-exploitation and use of oil resources, the world's oil resources are tending to be depleted, the problem of environmental pollution is becoming more serious, and exhaust emissions from internal combustion engines have become one of the most prominent environmental and socio-economic problems in the world, which has led to stricter emission regulations around the world [2–4]. As a consequence, potential alternative energy sources like ammonia, natural gas and hydrogen have been investigated to supplant these conventional fuels, where natural gas constitutes around 25% of primary energy share [5–10]. The use of clean and efficient alternative fuels such as natural gas in vehicle engines is a direct and effective way of reducing pollutants such as CO, NOx and PM [11–13]. Natural gas is a gas mixture. Its main component is methane (82–99% by volume), a simple hydrocarbon molecule composed of carbon and hydrogen [14]. Compared to diesel consumption of $0.273/km and petrol of $0.081/km, natural gas consumption is $0.047/km. Therefore, natural gas has huge potential economic and environmental benefits, the study of natural gas engines is of great practical importance [15–18].

As the compression ratio increases, the natural gas burns at a rapid rate and with high thermal efficiency [19, 20]. Due to their favorable H/C ratio, they can produce lower carbon-based emissions per unit of fuel than petrol [21–23]. Compared to natural gas, diesel fuel contains a complex mixture of long-chain hydrocarbons including sulfur, nitrogen and other impurities. These impurities can cause diesel to burn incompletely and produce large amounts of particulate matter. Natural gas engines can therefore emit less particulate matter than diesel engines [12,13]. Even under lean-burn conditions, natural gas engines can achieve lower carbon dioxide levels than diesel engines at approximately the same thermal efficiency [24–26].

* e-mail: kainany@163.com

At present, scholars are researching natural gas engines with consideration given to turbochargers. Kesgin [27] studied the effect of turbocharging system parameters on the performance of natural gas engines. It was shown that the selection of turbocharger with appropriate parameters can effectively improve the overall performance of the engine. In addition, Kesgin [28] also designed a two-stage high-pressure turbocharged natural gas engine and investigated the potential Miller cycle through calculations using computational models based on both experimental and computational studies. They also concluded that the efficiency of the engine was improved. Altosole et al. [29] applied a developed and validated computer simulator to a four-stroke marine natural gas engine to investigate the effects of the hybrid turbocharging system on the overall efficiency of the engine. They showed that the hybrid turbocharger had improved engine characteristics at different engine loads and speeds compared to the original engine. Luo et al. [30] investigated the compensation of low-speed performance of natural gas turbocharged engines based on the optimisation of the intake strategy, and obtained the conclusion that the use of a turbocharger can increase the efficiency of the engine by an average of 3.6%.

Due to the slow combustion speed of natural gas and poor lean-burn capability, the spark ignite (SI) engine has the disadvantage of large cycle-to-cycle variations and poor lean-burn capability, which reduces engine power and increases fuel consumption [31,32]. To solve the problem of power reduction in natural gas engines, turbocharging technology is often used to improve engine performance. The turbocharger compresses the intake air mixture by extracting waste energy from engine combustion emissions. Turbocharging then increases the power output of internal combustion engines and reduces specific fuel consumption [33]. However, at low engine speeds, there may not be enough exhaust gas flow to drive the turbine effectively, resulting in a decrease in turbine power [34]. Therefore, it is necessary to solve the turbocharger matching problem of natural gas engines. If the engine and turbocharger are not properly matched, the boost pressure often fails to reach the target value, resulting in suboptimal low-speed torque performance of natural gas engines [35,36].

For turbocharger system research, researchers focus mainly on building and improving models. The commercial software GT-Power, tailored for engine simulation, is used to build engine models [37,38]. The detailed geometry of the model, including lengths, diameters, junctions and topologies, is determined by the geometry of the engine. De Bellis et al. [39] built a turbocharger model with a scrap door, predicted the mass flow rate of the turbine inlet under different operating conditions based on the GT-Power turbine model, evaluated the steady-state flow performance of the turbine and verified it by experiment. Payri et al. [40] proposed a new physical model developed using basic physical principles and equations to calculate the hydrodynamic properties and energy conversion of the turbine of an internal combustion engine. Passar et al. [41] evaluated a new method for the design and estimation of turbine blade sections for turbocharged engines, and this technology provides a new direction for the subsequent evaluation of the interface geometric parameters of turbine blades. Yang et al. [42] established an analytical model of engine parameters and turbocharger system functions to study the main factors affecting turbocharger boost pressure and engine performance. Wahlström et al. [43] developed, parameterized and validated a mean value model of a diesel engine with variable geometry turbocharger (VGT) and exhaust gas recirculation (EGR) to predict the performance and behavior of diesel engines. By adjusting the model parameters and using optimization methods to capture the non-linear system dynamics, the accuracy of the model is improved. The available literature shows that many scientists have carried out in-depth research on turbocharger performance using modelling or computational methods. However, there is no systematic and in-depth research on the matching of turbocharger and engine. Therefore, it is of utmost importance to conduct comprehensive research on the matching of turbocharging systems for natural gas engines.

When matching the engine to the turbocharger, the first step is to select a suitable turbocharger. If the turbocharger is not selected correctly, the engine will not achieve the ideal level of power output and fuel efficiency. By establishing a mathematical model for engine-turbocharger matching and using computer simulation techniques, it is possible to speed up the development process while reducing the associated costs.

In this paper, the pre-matching method of engine and turbocharger is used to optimise the matching of turbocharger and natural gas engine based on the results of experimental data analysis. This paper is of great significance in guiding the performance development of turbocharged natural gas engines.

2 Numerical development of engine and turbocharger pre-matching

2.1 Pre-matching theory of engine and turbocharger system

The usual method of turbocharger selection is to input the performance map of the compressor and turbine into engine operating simulation software such as GT-Power to perform complex calculations. This method, which requires a large database of performance maps, is not only complex but also very time consuming. In addition, in the early stages of engine design, this method does not provide an intuitive assessment of the parameters required to achieve the engine performance goals, such as the required airflow, boost pressure, etc. This is also the reason why many of the turbochargers matched by this method do not meet the requirements. Therefore, a self-developed software for dedicated turbocharger pre-matching is proposed and subsequent parameter settings are performed in this software. The pre-matching method used in this paper is based on the target performance of the engine, given known parameters such as the number of engine cylinders, the number of strokes, the displacement and the external characteristic torque, etc. Thus, the turbocharger pressure ratio and mass flow to match the engine power can be

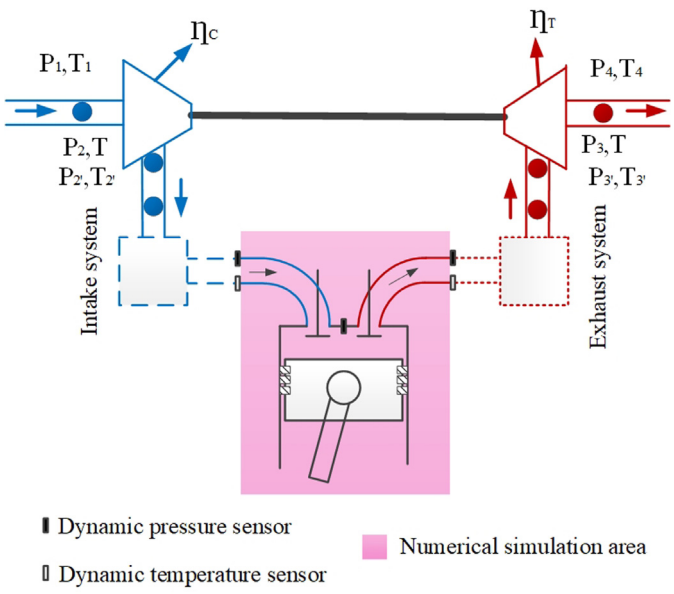

Fig. 1. Schematic diagram of turbocharging system parameters.

obtained from the engine displacement, external characteristic torque, etc. In this way, the flow characteristic can be obtained to find an intuitive and a priori condition for matching the engine and the turbocharger. It is a quick and effective way to find one or more suitable turbochargers through this a priori condition to complete the pre-matching. The schematic diagram of the turbocharging system parameters is shown in Figure 1.

The power absorbed by turbine end impeller as follows:

$$P_T = \dot{m}_3 C_{P_3} T_3 \left[1 - \left(\frac{P_4}{P_3}\right)^{\frac{\gamma_3 - 1}{\gamma_3}}\right] \eta_T, \tag{1}$$

where P_T is the power of the turbine, m_3 is the mass flow of the exhaust gases through the turbine, C_{P_3} is the specific heat of the exhaust gases at constant pressure, T_3 is the temperature at the turbine exhaust gas outlet, P_3 is the pressure at the turbine gas inlet, P_4 is the pressure at the turbine gas outlet, γ_3 is the specific ratio of the exhaust gases, η_T is the adiabatic efficiency of the turbine.

The power consumed by compressor end impeller as follows:

$$P_C = \frac{\dot{m}_1 C_{P_1} T_1 \left[\left(\frac{P_2}{P_1}\right)^{\frac{\gamma_1 - 1}{\gamma_1}} - 1\right]}{\eta_C}, \tag{2}$$

where P_C is the power of the compressor, $\dot{m}_1$ is the mass flow of the suction gases through the compressor, CP_1 is the specific heat at constant inlet pressure, T_1 is the temperature of the compressor before the compressor inlet, P_1 is gas inlet pressure of the compressor, P_2 is the gas outlet pressure of the compressor, γ_1 is the specific ratio of the air, n_C is the adiabatic efficiency of the compressor.

when the turbocharger reaches a power balance condition, the power at both ends of the turbocharger is balanced as follows:

$$P_T \eta_m = P_C, \tag{3}$$

where η_m is the mechanical efficiency of the drive shaft.

Thus, the power balance equation of the turbocharger can be expressed by the following equation:

$$\dot{m}_3 C_{P_3} T_3 \left[1 - \left(\frac{P_4}{P_3}\right)^{\frac{\gamma_3 - 1}{\gamma_3}}\right] \eta_T \eta_m = \frac{\dot{m}_1 C_{P_1} T_1 \left[\left(\frac{P_2}{P_1}\right)^{\frac{\gamma_1 - 1}{\gamma_1}} - 1\right]}{\eta_C}. \tag{4}$$

The gas mass flow through the turbine end under power balance conditions is equal to the gas mass flow at the compressor end plus the fuel mass flow:

$$\dot{m}_3 = \dot{m}_1 + \dot{m}_{fuel}, \tag{5}$$

where $\dot{m}_{fuel}$ is the mass flow of fuel.

Since the turbine end and the turbocharger end are rigidly connected by a connecting shaft, the speed ratio between the turbine and the compressor is as follows:

$$n_T = n_C, \tag{6}$$

where n_T is the speed of the turbine, n_C is the speed of the compressor.

Applying the equations (1)–(6), the relationship between the flow rate and pressure ratio of the compressor meeting the torque demand of the engine can be expressed by equation (7):

$$\frac{P_3}{P_4} = \frac{1}{1 - \left\{\frac{\dot{m}_1 C_{P_1} T_1}{\dot{m}_3 C_{P_3} T_3 \eta_T \eta_m \eta_C}\left[\left(\frac{P_2}{P_1}\right)^{\frac{\gamma_1 - 1}{\gamma_1}} - 1\right]\right\}^{\frac{\gamma_3 - 1}{\gamma_3}}}. \tag{7}$$

Specific information on equations (1)–(7) can be found in related literature [44].

2.2 Pre-matching method of engine and turbocharger system

In general, the matching of engine and turbocharger has three aspects: the matching of engine and compressor, the matching of engine and turbine and the matching of compressor and turbine. The basic idea of the method is described in detail below. Typically, the volumetric flow value is between 0 and 1, while the pressure ratio is between 1 and 3.

2.2.1 Compressor map definition

– Defines the surge line. The compressor map parameter definition diagram as shown in Figure 2 and the four blue points from bottom left to top right are defined as surge

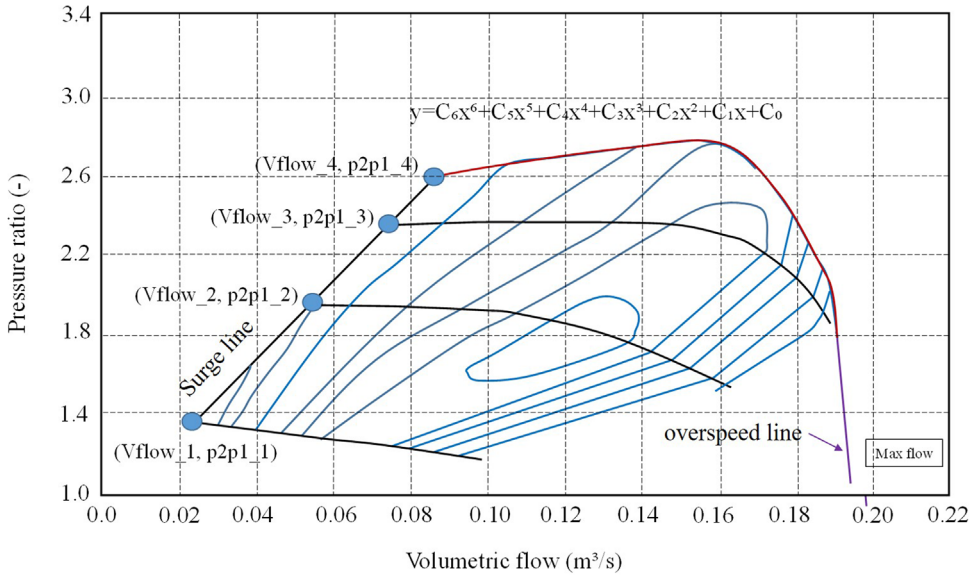

Fig. 2. Compressor flow map.

point 1 (Vflow_1, p2p1_1), point 2 (Vflow_2, p2p1_ 2), point 3 (Vflow_3, p2p1_3) and point 4 (Vflow_4, p2p1_4), whose coordinates are known.

– Defines the overspeed line. Select the maximum constant speed line of the compressor and fit a sixth order equation, which is the overspeed line equation. The equation form is $y=C_6x^6+C_5x^5+C_4x^4+C_3x^3+C_2x^2+C_1x+C_0$, and specific C_6, C_5, C_4, C_3, C_2, C_1, C_0 is the coefficient of the sixth order equation.
– Define the maximum flow. The intersection of the overspeed line extension (purple) and the X-axis is defined as the maximum flow of the compressor.

2.2.2 Compressor matching algorithm and process

Turbocharger matching technology involves selecting a suitable compressor and turbine for the turbocharger system based on the results of the matching calculation. The compressor matching selection process is shown in Figure 3, where Cmp_max_flow = Max{Vflow_1, Vflow_2, Vflow_3, Vflow_4,}.

The exact calculation process is shown below:

– If Cmp_Vflow > Vflow_4, substituting Cmp_Vfolw into the overdrive equation to calculate p2p1;
– If Cmp_Vflow < Vflow_1, substituting Cmp_Vfolw into the equation p2p1(L) + (Cmp_Vflow − Vflow_(L)) * (p2p1_ (L+1)-p2p1_ (L))/(Vflow_ (L+1)-Vflow_ (L)) to calculate p2p1;
– If Cmp_Vflow < Vflow_1, calculating p2p1 by substituting Cmp_Vfolw into the linear equation determined by points (2, 1) and (Vflow_1, p2p1_1).

2.2.3 Turbine map definition

The curve on the turbine map plot was selected and a sixth order equation of the form $y= C_6x^6 + C_5x^5 + C_4x^4 + C_3x^3 + C_2x^2 + C_1x + C_0$ was fitted, where specific C_6, C_5, C_4, C_3, C_2, C_1, C_0 are the coefficients of the sixth order equation. Figure 4 shows that the volumetric flow initially increases with the pressure ratio and the curve reaches a convergent state when the pressure ratio is 2.2. It can also be seen that the turbine has a large flow capacity so that it is not easily clogged at high engine speeds. The point of maximum flow and pressure ratio is defined as (Max_pratio, Max_redflow) as shown in Figure 4.

2.2.4 Turbine matching algorithms and processes

The turbine matching selection process is shown in Figure 5, where δ(tur_redflow) and δ(tur_map_data) denote the relative errors of tur_redflow and tur_map_data, respectively. When performing the turbocharger parameter calculation, the basic engine parameters are first entered into the basic parameters section of the software. The associated parameters are then entered into the engine operating point definition section of the software. The engine operating points are given in Table 1, where PMEP and FMEP are abbreviations for friction mean effective pressure and pumping mean effective pressure.

3 The research of turbocharger performance experiment

A comprehensive performance test of a turbocharger has been carried out, including a turbine characteristic test and a compressor characteristic test. The performance of the turbocharger can be comprehensively evaluated. Combined with the results of the experimental data analysis, the matching of the turbocharger and the natural gas engine can be optimised through the development of the turbocharger pre-matching method and the use of the analytical method.

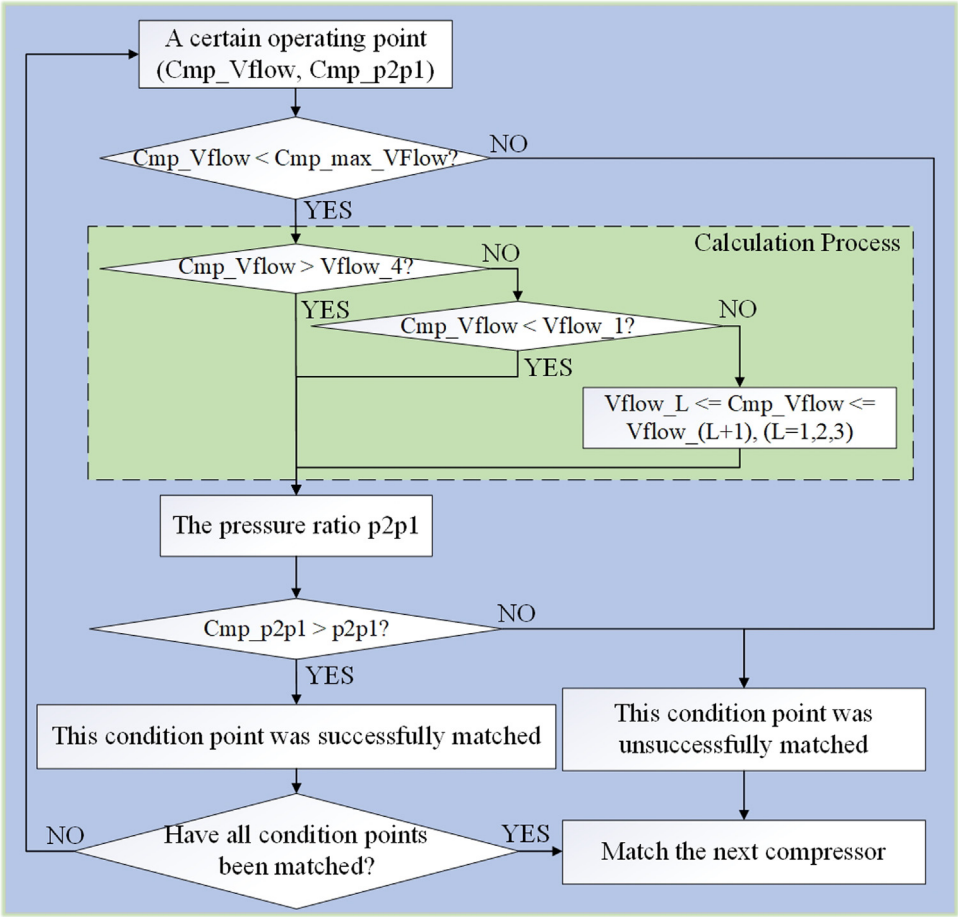

Fig. 3. Developed compressor matching process.

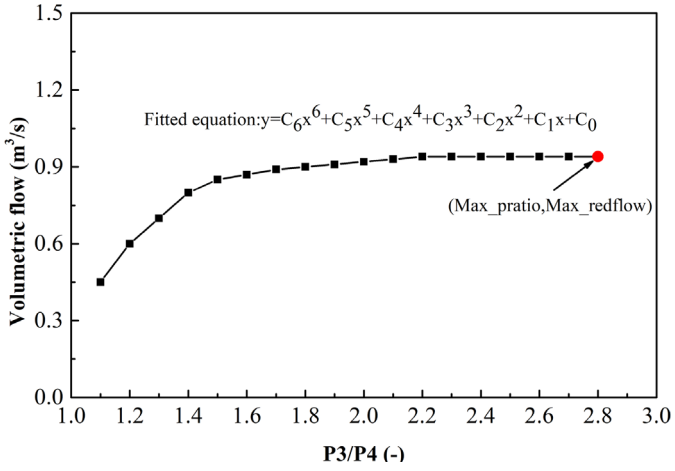

Fig. 4. Turbine map.

3.1 Experimental facility

The test object is a HOLSET HX40G turbocharger and the technical parameters of the corresponding natural gas engine are shown in Table 2.

The experiment was carried out on a special test bench for turbine and compressor characteristics. The temperature, pressure, speed and other experimental parameters are controlled according to the relevant provisions of GB/T 23341.2-2009 [45]. For example, the environmental conditions inside the test room were controlled at the standard status, namely the air temperature is 25 ± 1 °C, the pressure is 101.3 ± 0.1 kPa, and the humidity was monitored throughout the test process (for emission correction if necessary). And the intercooler temperature at the rate power point was controlled within ± 5 °C as specified by the manufacturer, and it cannot be lower than 20 °C. The main sensor arrangement during the experiment is shown in Figures 6 and 7. The compressed air flows through the air filter and the eddy current flowmeter to reach the combustion chamber where it ignites the injected fuel. The combustion exhaust then drives the turbine. The compressor, which is rigidly connected to the turbine by a connecting shaft, is also driven. Meanwhile, the speed of the compressor is measured by a speed sensor and fed into the computer. In addition, the oil tank plays a role in lubricating the booster circuit, while the emission control system and the intake control system are responsible for controlling the gas flow. The test bench test and measurement equipment is shown in Table 3.

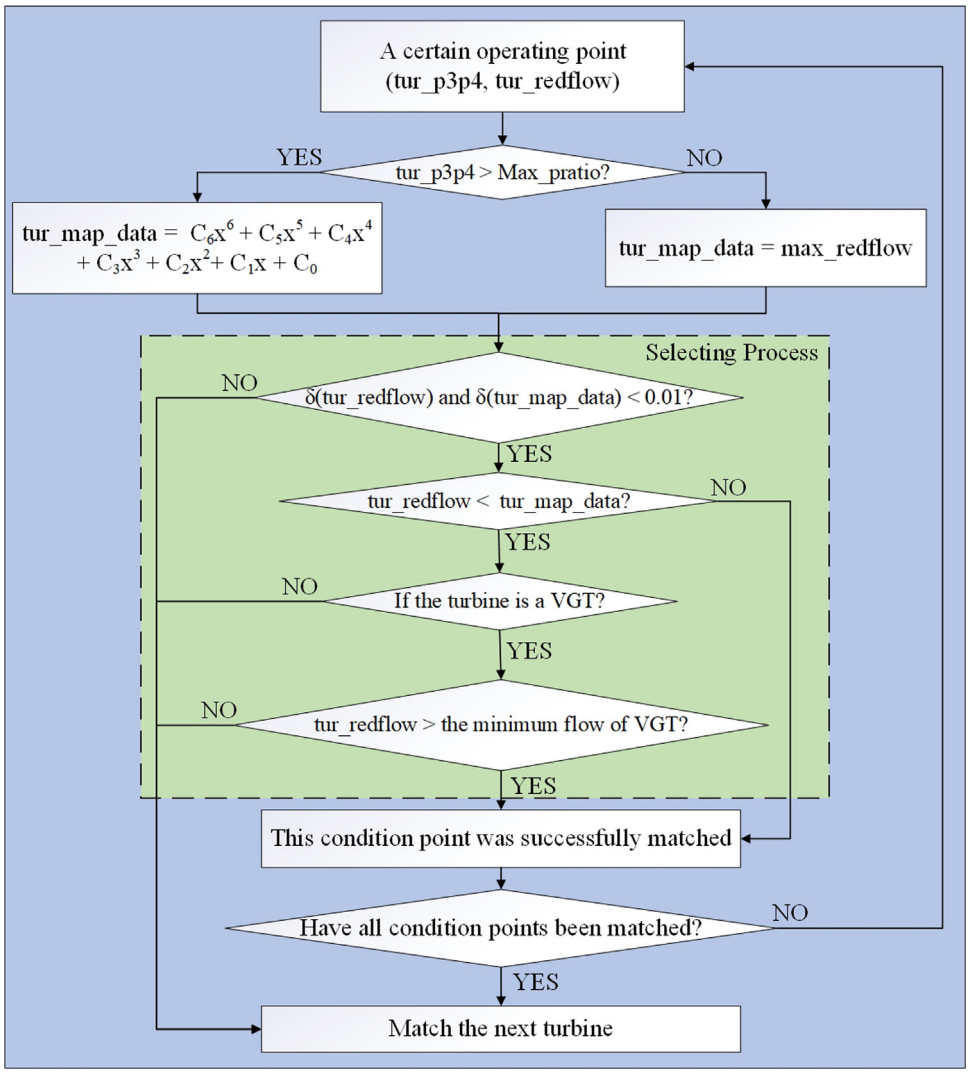

Fig. 5. Developed turbine matching process.

Table 1. Definition of engine operating points.

Condition number (–)	Speed (r/min)	PMEP (bar)	Excess air coefficient (–)	FMEP (bar)	Charging efficiency (–)	Turbine efficiency (%)	Compressor efficiency (%)	Intercooling efficiency (%)	Power (kW)
1	1000	10	1.3	1	0.87	62	69.5	80	20.83
2	2000	18.09	1.371	1.7	0.89	62	74	80	75.36
3	2500	17.9	1.407	1.84	0.9	63	75.5	80	93.21
4	3000	16.5	1.443	2.1	0.84	64	68	80	103.1
5	4000	13.8	1.5	2.7	0.8	65	67.5	80	115

3.2 The analysis of experimental result

According to the experimental results, the flow and efficiency characteristics of the turbine and compressor are shown in Figures 8a–8d, respectively. It can be seen from Figure 8b that the turbine can reach a maximum efficiency of about 70% at a speed of 6000 rpm and a pressure ratio of 1.25. The high efficiency range (>67.5%) of this turbine is in the low pressure ratio range (1.25-1.5) and this turbine is suitable for matching the engine with lower lift power, which is more suitable for working under the low load of the engine. As the pressure ratio of this turbine increases at different speed conditions, the efficiency decreases significantly, which may result in insufficient engine power. Furthermore, Figure 8d shows that this compressor can reach a maximum efficiency of

Table 2. Main engine parameters.

Item	Natural gas engine parameters
Number of cylinders	6
Displacement	10L
Rated power	247kW/2200rpm
Ignition order	1–5–3–6–2–4
Rated fuel consumption rate	195g/(kWh)
Maximum no-load speed	2500 ± 50 r/min
Minimum steady rate of operation	600 ± 50 r/min
Turbine rear exhaust temperature	580 °C
Noise	93 dB

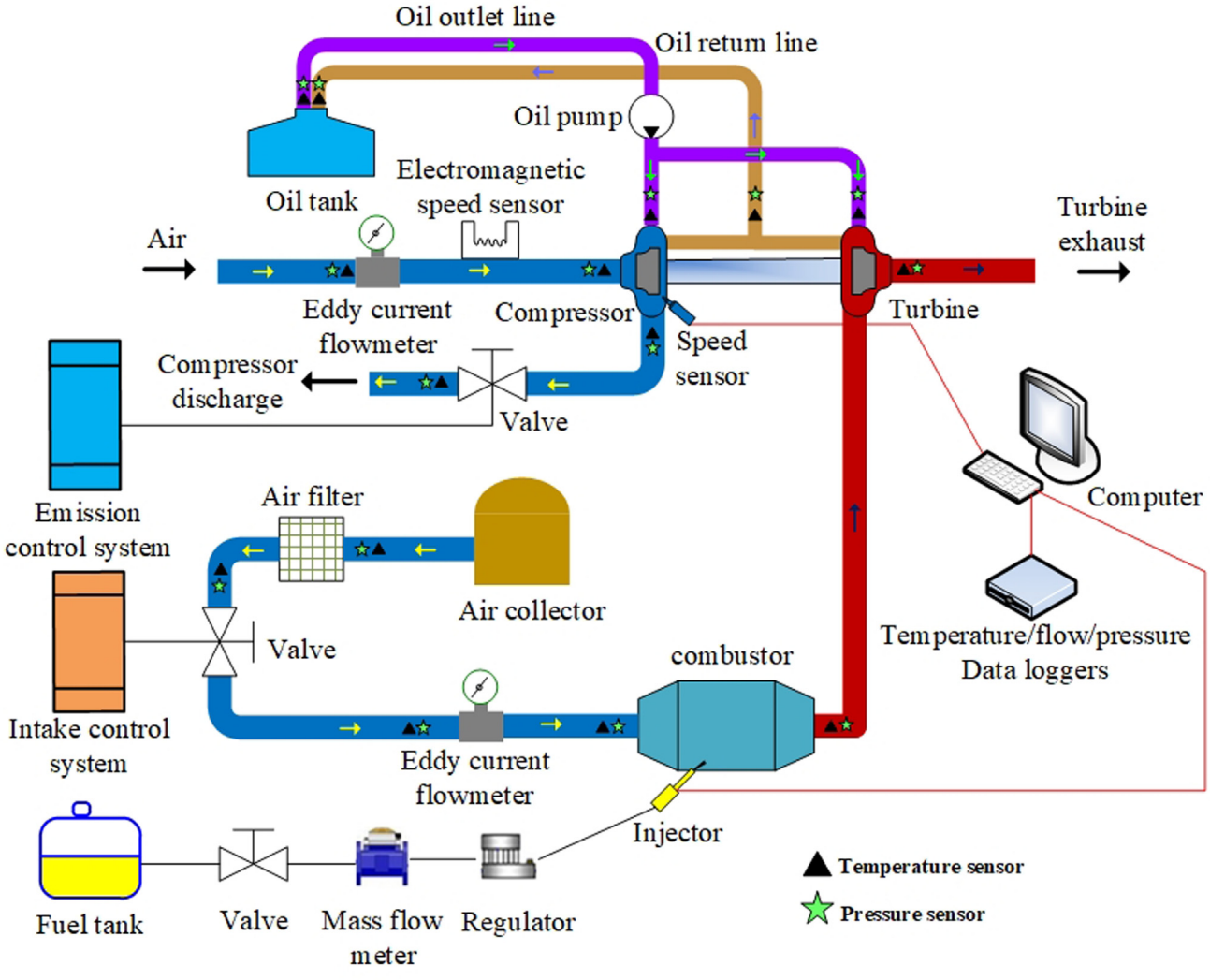

Fig. 6. The schematic diagram of turbocharger test bench.

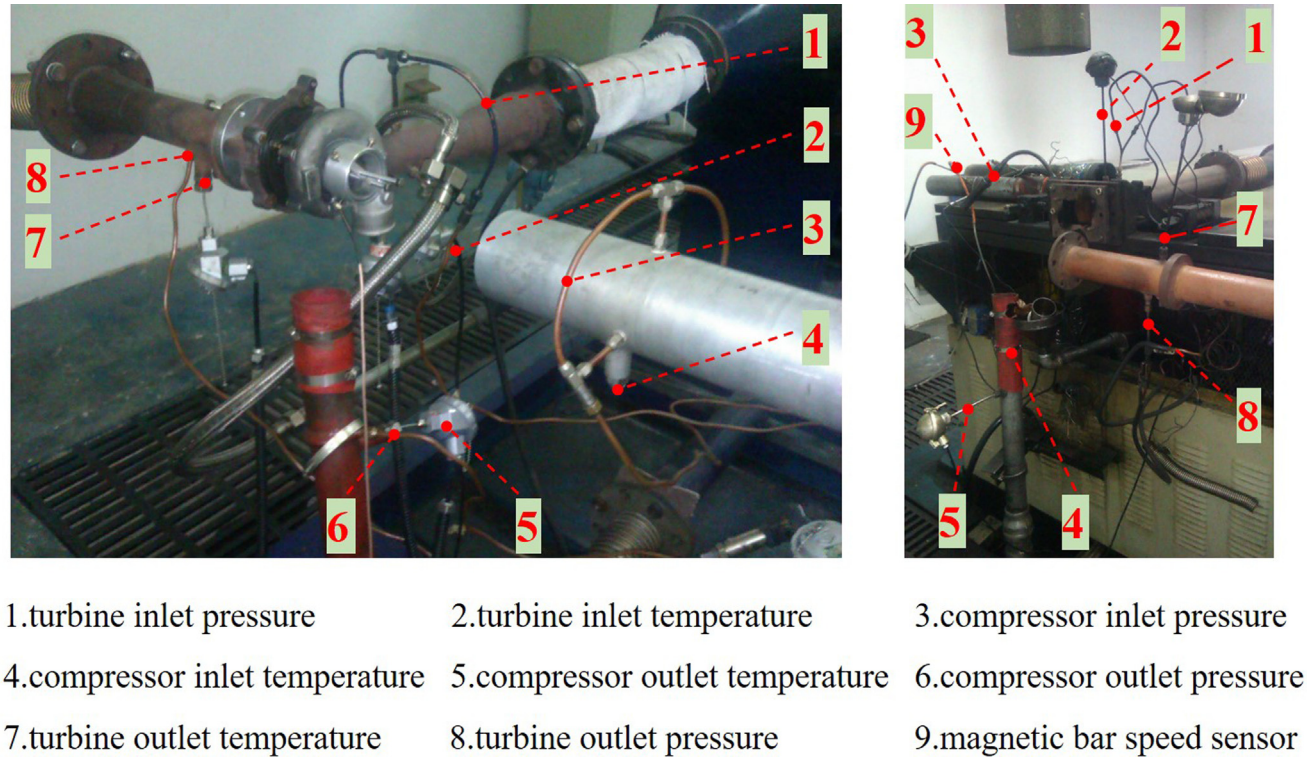

Fig. 7. Turbine and compressor characteristic experiment sensor arrangement.

Table 3. Bench test equipment and measuring equipment.

Equipment name	Manufacturer/type	Measurement range	Accuracy
Eddy current flowmeter	TOCEIL-CMF025 (Shanghai ToCeil Engine Testing Equipment Co., LTD. Shanghai, China)	0–60 L/min	±0.35%
Speed sensor	CP-044 (Guangzhou Jichuang Electronic Equipment Co., LTD. Guangzhou, China)	400–6000 rpm	0.5%
Temperature sensor	PT100 (Hunan Xiangyi Dynamic Testing Instrument Co., LTD. Changsha, China)	0–300 °C	±0.15 °C
Pressure sensor	Piezoresistive transducer (Hunan Xiangyi Dynamic Testing Instrument Co., LTD. Changsha, China)	0–3.5 bar	0.1% FS
Air filter meter	Lambda square orifice plate	0–500 CFM	0.1%

about 75% at a speed of 10 000 rpm and a mass flow of 0.40 kg/s. In addition, the equivalent flow is equal to the mass flow multiplied by the square root of the temperature and divided by the pressure.

According to the given engine parameters and the measured compressor map, the engine and turbocharger were pre-matched and analysed. The pre-matching map of engine and compressor is obtained as shown in Figure 9. The operating point of the engine is predicted by the provided engine parameters and the compressor map is entrusted to a turbocharger manufacturer for actual measurement.

The analysis and evaluation of the matching performance of engine and turbocharger can lead to the following conclusions:

– The highest efficiency zone of the compressor falls in the high pressure ratio area, and the highest efficiency zone of the turbine falls in the low pressure ratio area, indicating that the compressor and turbine are poorly matched.
– The highest efficiency zone of the compressor falls in the high pressure ratio area, and the operating points of the engine fall in the area where the compressor efficiency is lower, indicating that this engine cannot fully utilize the high efficiency of the compressor during operation.

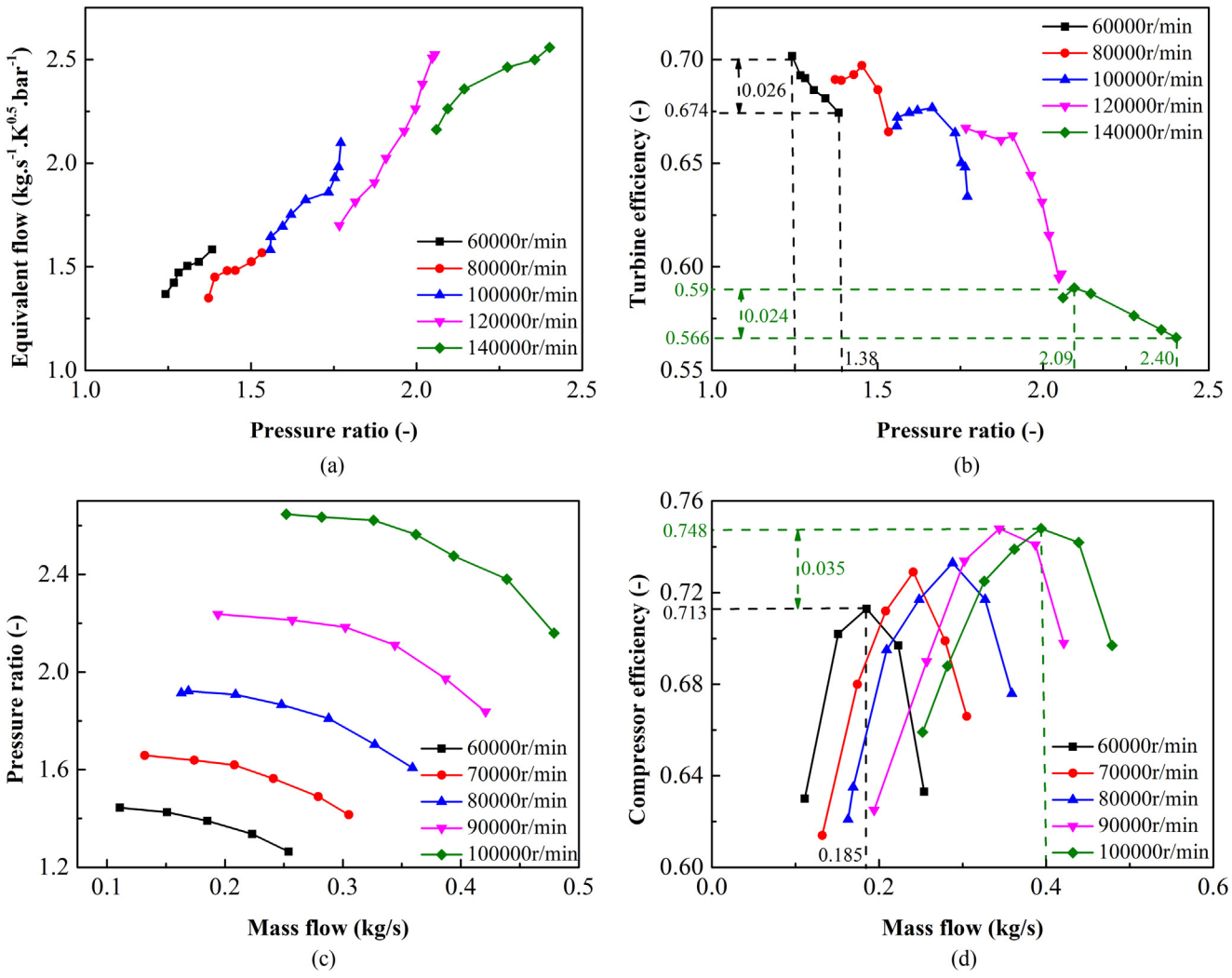

Fig. 8. Characteristic curves of the turbine and compressor.

– As can be seen from Figure 9, the operating condition of the engine has enough margin from the surge line and the drag line. In addition, the high speed and blockage area maintain a certain distance, and the turbocharger will not be surge and blockage.
– The entire engine operating line is to the left of the compressor curve, indicating that the engine corresponds to the lower compressor efficiency at low speeds, and the proximity to the surge area leads to the possibility of surge.

4 The analysis and comparison of turbocharger performance

4.1 The comparison of compressor matching

Compressors #1, #2 and #3 in the developed database were selected to rematch the engine and the pre-matched map of the engine and compressors is shown in Figures 10–12, respectively. After the engine was pre-matched with these three turbochargers, it can be seen from the figure that the low-speed point is a certain distance away from the surge line, and the high-speed point has plenty of margin from the blocking line, and neither of them exceeds the surge line and the blocking line. The maximum efficiency of the compressor reaches the 77–79% efficiency region, which means that the engine operating condition point falls in the higher efficiency region of the compressor, which is conducive to the reduction of pumping losses, thus improving the engine's power performance and the engine's economy. Therefore, when the engine is rematched with the three turbochargers, the engine operating points fall into the higher efficiency zone of compressors #1, #2 and #3, which is conducive to reducing pump air losses and thus improving the power output of the engine.

4.2 The analysis of turbine comparation

It can be seen from the previous turbine characteristic experiment that the maximum efficiency of the turbine is 70% and the efficiency of the turbine decreases significantly as the pressure ratio increases. The flow characteristics of turbines #1, #2 and #3 selected from the developed

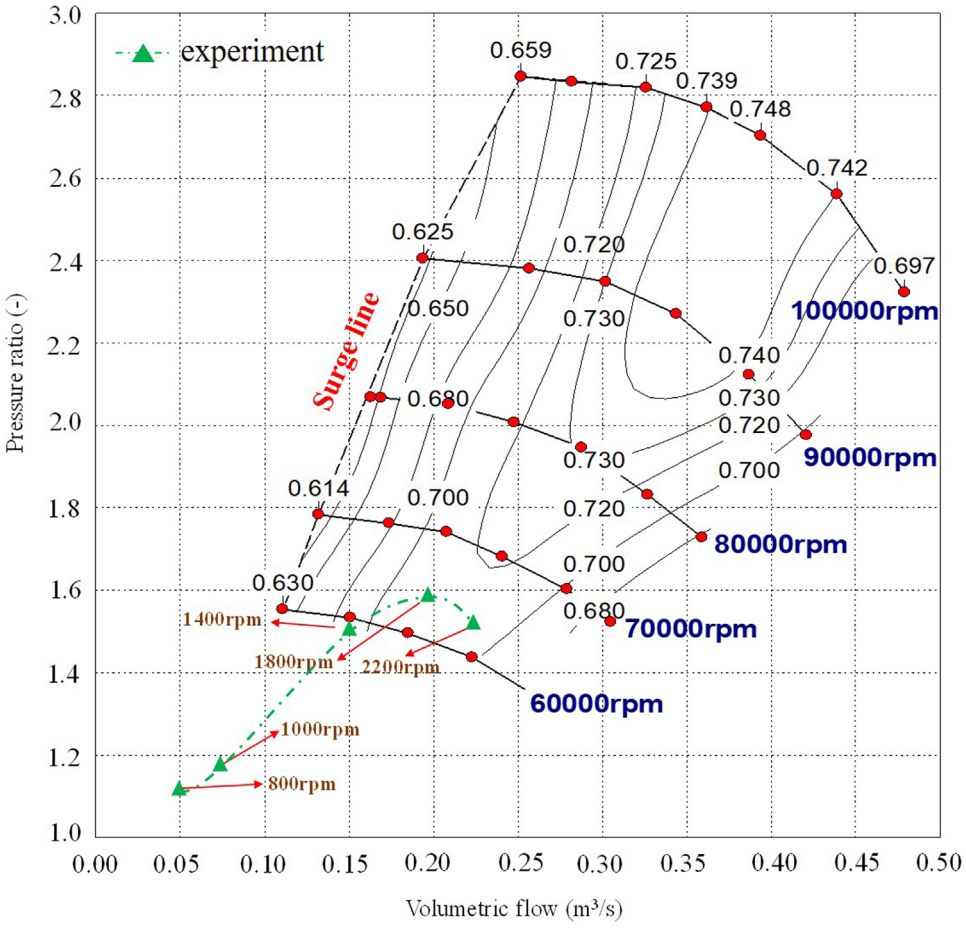

Fig. 9. Pre-matching map of the engine and compressor.

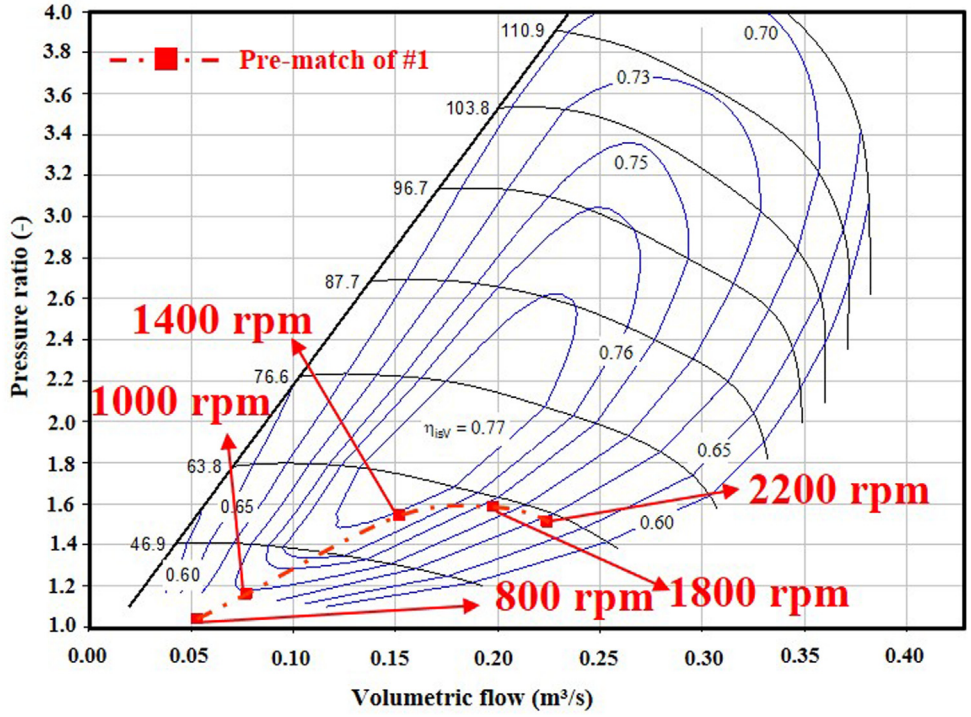

Fig. 10. Pre-matching map of the engine and the #1 compressor.

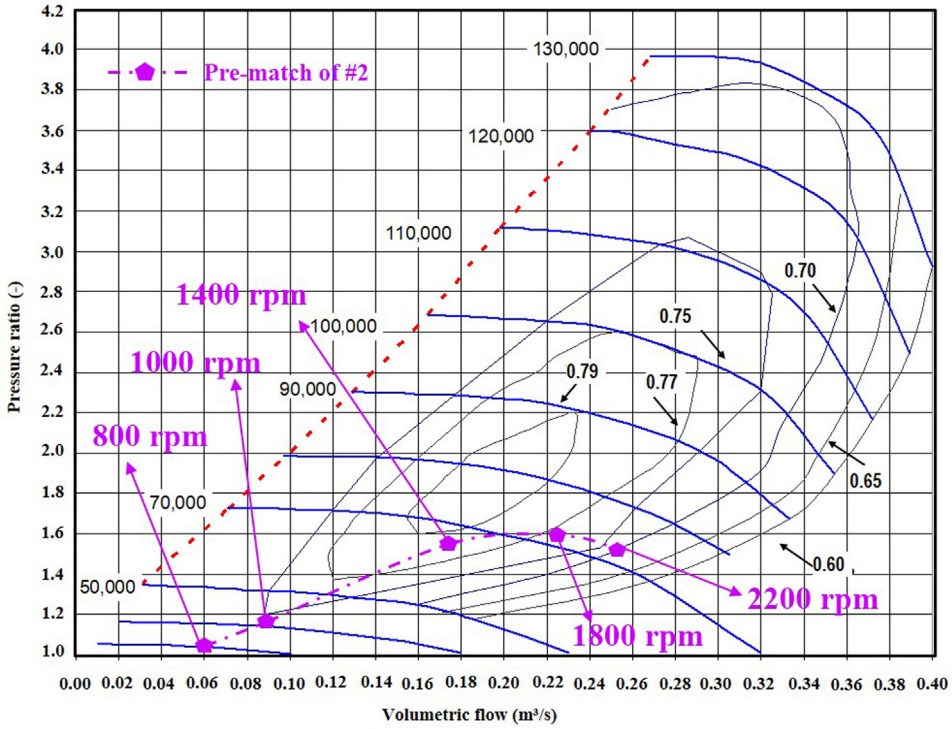

Fig. 11. Pre-matching map of the engine and the #2 compressor.

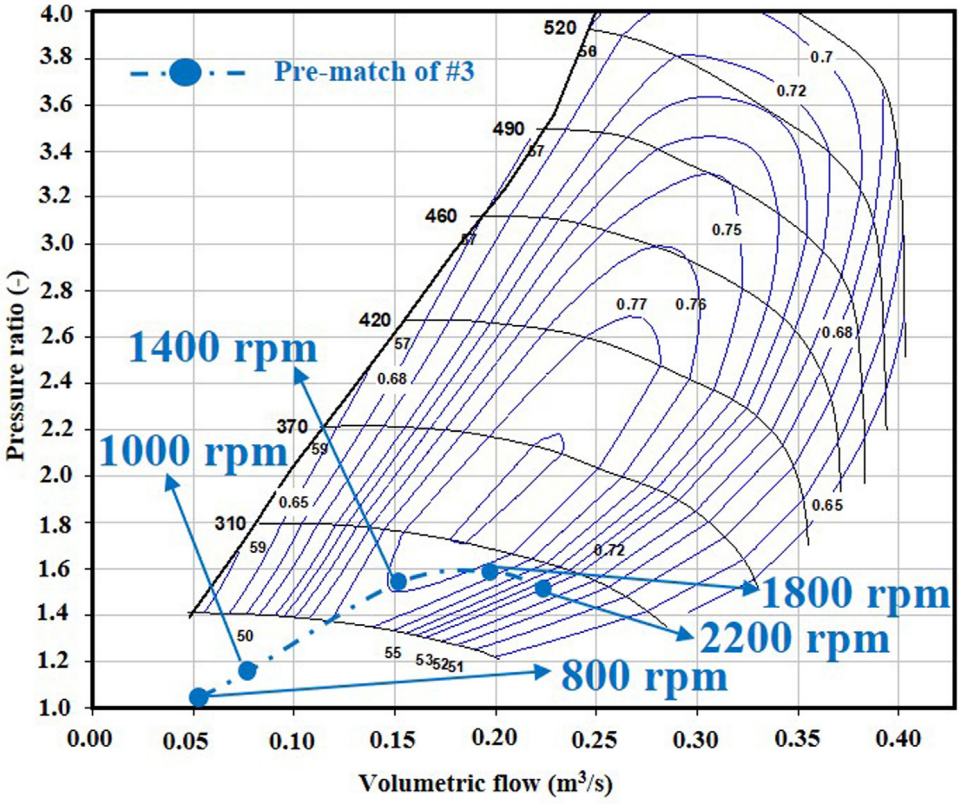

Fig. 12. Pre-matching map of the engine and the #3 compressor.

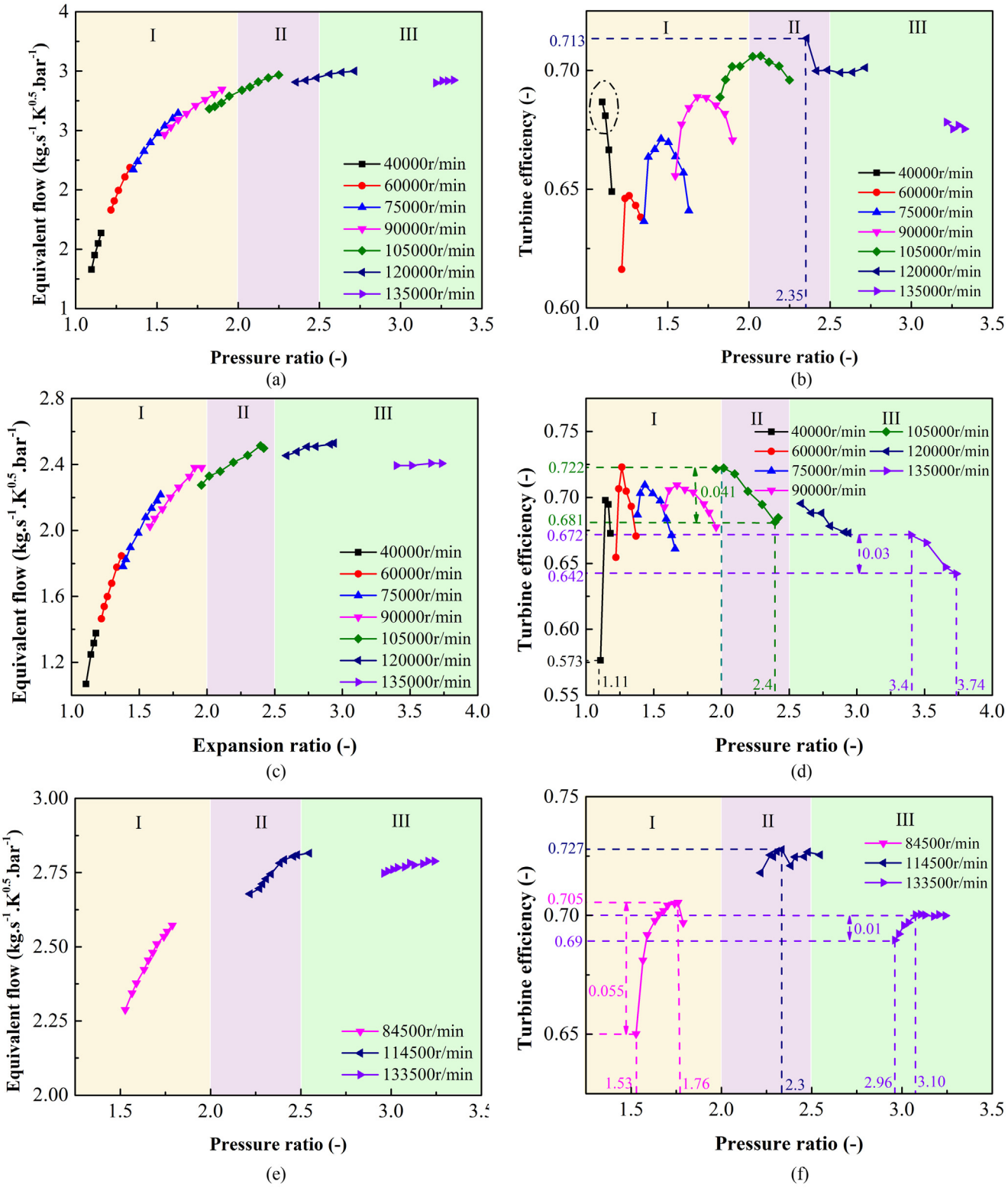

Fig. 13. Characteristic curve of the three turbines.

database show that the flow increases as the pressure ratio increases and finally converges to a certain value as shown in Figures 13a, 13c and 13e. In addition, the efficiency of these three turbines in the database can maintain a stable and relatively high efficiency (>65%) over a wide range of pressure ratios (1.5–3.5). It can be seen from Figures 13b, 13d and 13f that the maximum efficiencies of turbines #1, #2 and #3 are 71.3%, 72.2% and 72.7% respectively and that there is a decreasing tendency for the turbine efficiencies to vary with pressure ratio as the speed increases. Since the turbine pressure ratio must be greater than 1, the experiment is unstable when the turbine pressure ratio is 1. Therefore, turbine #1 did not perform the experiment when the pressure ratio is 1 at a speed of 40000 r/min, as shown in Figure 13b. According to the characteristics of these three turbine curves, the pressure ratio is divided into three regions: Region I (1.0–2.0), Region II (2.0–2.5) and Region III (>2.5). At the same time, it can be seen from Figure 13f that turbine #3 can achieve maximum efficiency at a speed of 114500 rpm (Region II). The efficiency curves of turbines #1 and #2 also reach maximum efficiency in region II, as shown in Figures 13b and 13d respectively. This means that there is not a simple linear relationship between pressure ratio and turbine efficiency, and that higher pressure ratios and speeds do not contribute more to efficiency.

Turbine #2 or #3 in the database can be selected to improve the torque and transient response of the engine at low speed, while turbine #1 can be selected to improve the matching of the engine at high speed and reduce fuel consumption. The results of the comparative analysis show that the matching of turbocharger and engine can be optimized according to the requirements, and the engine performance can be further improved by the rational selection of the turbocharger.

5 Conclusion

In this paper, the turbocharger pre-matching calculation and analysis are carried out according to the engine performance parameters and turbocharger performance measurement data. The matching method of engine and turbocharger is developed based on the numerical development technology, and the three turbines and three compressors included in the software database were re-matched, compared and analyzed. Through these experiments, the following conclusions are obtained:

- Based on the self-developed software dedicated to pre-matching, a pre-matching method was proposed. In this method, the subsequent work and time required for matching can be reduced, and many parameters of the engine can be seen directly, which can facilitate the subsequent design.
- According to the analysis of the turbine characteristic experiment and the compressor characteristic experiment, the turbine can achieve a maximum efficiency of about 70%. When the pressure ratio of this turbine increases, the efficiency decreases significantly, which may lead to insufficient engine performance.
- Three different compressors and three turbines were selected from the matching software database for further comparative analysis. The efficiency of these three turbines in the database can maintain a stable and relatively high efficiency (>65%) over a wide range of pressure ratios (1.5–3.5). The maximum efficiencies of the 1#, 2# and 3# turbines are 71.3%, 72.2% and 72.7% respectively, and the trend of the turbine efficiencies with changing pressure ratios becomes smaller and smaller with increasing speed. The turbine efficiency is more stable at higher speeds.
- Compared with the traditional method, the maximum efficiency of the turbine has increased by 1–3% and the overall efficiency has improved after the pre-matching. The pre-matching method can optimize a large part of the engine operating range and almost all probable operating points during a duty cycle to achieve maximum efficiency for both compressor and turbine.

Nomenclature

EGR	Exhaust gas recirculation
FMEP	Friction mean effective pressure
GB/T	China national standard
PMEP	Pumping mean effective pressure
SI	Spark Ignite
VGT	Variable geometry turbocharger

Acknowledgements

The authors appreciate the reviewers and the editor for their careful reading and many constructive comments and suggestions on improving the manuscript.

Funding

This research work is jointly sponsored by National Key Research and Development Program of China (2022YFB3403200), Hunan Provincial Natural Science Foundation of China (2023JJ41056), Hunan Provincial Department of Education Project, China (21B0273) and the Scientific Innovation Fund for Postgraduates of Central South University of Forestry and Technology (2022CX02072).

Author's contribution

Feng Zhou: Conceptualization, Software, Validation, Writing Original draft, Methodology; Zichao Meng: Writing Review & Editing, Formal analysis, Investigation; Xu Xiao: Writing Review & Editing, Data curation; Jianqin Fu: Supervision, Project administration; Kainan Yuan: Formal analysis, Conceptualization, Funding acquisition; Zhuangping Cui: Conceptualization, Resources; Juan Yu: Visualization; Jingping Liu: Formal analysis.

References

[1] M.A. Kurgankina, G.S. Nyashina, P.A. Strizhak, Prospects of thermal power plants switching from traditional fuels to coal-water slurries containing petrochemicals, Sci. Total Environ. **671**, 568–577 (2019)

[2] J.P. Szybist, R.R. Steeper, D. Splitter, V.B. Kalaskar, J. Pihl, C. Daw, Negative valve overlap reforming chemistry in low-oxygen environments, SAE Int. J. Engines **7**, 418–433 (2014)

[3] V.S. Midhun, S. Karthikeyan, S. Krishnan, S.D. Rairikar, K.P. Kavathekar, S.S. Thipse, N.V. Marathe, Development of CNG injection engine to meet future euro-v emission norms for LCV applications, SAE Technical Paper No. 2011 26–0002

[4] D.S. Khatri, P. Rungta, Development and evaluation of a multipoint gas injection system for a passenger car, SAE Technical Paper No. 2008 – 28–0067

[5] G.T. Chala, A.R. Abd Aziz, F.Y. Hagos, Natural gas engine technologies: challenges and energy sustainability issue, Energies **11**, 2934 (2018)

[6] T. Hesterberg, W. Bunn, C. Lapin, An evaluation of criteria for selecting vehicles fueled with diesel or compressed natural gas, Sustain.: Sci. Pract. Policy **5**, 20–30 (2009)

[7] Y. Matsuo, A. Yanagisawa, Y. Yamashita, A global energy outlook to 2035 with strategic considerations for Asia and Middle East energy supply and demand interdependencies, Energy Strateg. Rev. **2**, 79–91 (2013)

[8] T. Cai, D. Zhao, Effects of fuel composition and wall thermal conductivity on thermal and NOx emission performances of an ammonia/hydrogen-oxygen micro-power system, Fuel Process. Technol. **209**, 106527 (2020)

[9] Y. Sun, T. Cai, M. Shahsavari, D. Sun, X. Sun, D. Zhao, B. Wang, RANS simulations on combustion and emission characteristics of a premixed NH3/H2 swirling flame with reduced chemical kinetic model, Chinese J. Aeronaut. **34**, 17–27 (2021)

[10] T. Cai, D. Zhao, Y. Sun, S. Ni, W. Li, D. Guan, B. Wang, Evaluation of NOx emissions characteristics in a CO_2-free micro-power system by implementing a perforated plate, Renew. Sust. Energ. Rev. **145**, 111150 (2021)

[11] B. Deng, Z. Chen, C. Sun, S. Zhang, W. Yu, M. Huang, K. Hou, J. Ran, L. Zhou, C. Chen, X. Pan, Key design and layout factors influencing performance of three-way catalytic converters: experimental and semidecoupled numerical study under real-life driving conditions, J. Clean. Prod. **425**, 138993 (2023)

[12] T.W. Hesterberg, C.A. Lapin, W.B. Bunn, A comparison of emissions from vehicles fueled with diesel or compressed natural gas, Environ. Sci. Technol. **42**, 6437–6445 (2008)

[13] E.R. Jayaratne, Z.D. Ristovski, N. Meyer, L. Morawska, Particle and gaseous emissions from compressed natural gas and ultralow sulphur diesel-fuelled buses at four steady engine loads, Sci. Total Environ. **407**, 2845–2852 (2009)

[14] V.N. Gamezo, R.K. ZipfJr, M.J. Sapko, W.P. Marchewka, K.M. Mohamed, E.S. Oran, D.A. Kessler, E.S. Weiss, J.D. Addis, F.A. Karnack, D.D. Sellers, Detonability of natural gas-air mixtures, Combust. Flame **159**, 870–881 (2012)

[15] J.C. Peters, Natural gas and spillover from the US Clean Power Plan into the Paris Agreement, Energ. Policy **106**, 41–47 (2017)

[16] S.H. Pourhoseini, R. Asadi, An experimental study on thermal and radiative characteristics of natural gas flame in different equivalence ratios by chemiluminescence and IR photography methods, J. Nat. Gas Sci. Eng. **40**, 126–131 (2017)

[17] R. Aloui, M.S.B. Aïssa, S. Hammoudeh, D.K. Nguyen, Dependence and extreme dependence of crude oil and natural gas prices with applications to risk management, Energ. Econ. **42**, 332–342 (2014)

[18] R.Z. Ríos-Mercado, C. Borraz-Sánchez, Optimization problems in natural gas transportation systems: a state-of-the-art review, Appl. Energ. **147**, 536–555 (2015)

[19] F. Zhou, J. Fu, D. Li, J. Liu, C.F. Lee, Y. Yin, Experimental study on combustion, emissions and thermal balance of high compression ratio engine fueled with liquefied methane gas, Appl. Therm. Eng. **161**, 114125 (2019)

[20] H. X, J. Fu, F. Zhou, J. Yu, J. Liu, Z. Meng, Experimental and numerical studies of thermal power conversion and energy flow under high-compression ratios of a liquid methane engine (LME), Energy **284**, 128544 (2023)

[21] L. Zhu, Z. He, Z. Xu, X. Lu, J. Fang, W. Zhang, Z. Huang, In-cylinder thermochemical fuel reforming (TFR) in a spark-ignition natural gas engine, P. Combust. Inst. **36**, 3487–3497 (2017)

[22] B. Deng, Q. Li, Y. Chen, M. Li, A. Liu, J. Ran, Y. Xu, X. Liu, J. Fu, R. Feng, The effect of air/fuel ratio on the CO and NOx emissions for a twin-spark motorcycle gasoline engine under wide range of operating conditions, Energy **169**, 1202–1213 (2019)

[23] S.A. Sobiesiak, S. Zhang, The first and second law analysis of spark ignition engine fuelled with compressed natural gas, SAE Technical Paper No. 2003 – 01–3091

[24] P.L. Mtui, P.G. Hill, Ignition delay and combustion duration with natural gas fueling of diesel engines, SAE Technical Paper No. 961933 (1996)

[25] R. Tilagone, G. Monnier, A. Chaouche, Y. Baguelin, S. De Chauveron, Development of a high efficiency, low emission SI-CNG bus engine, SAE Technical Paper No. 961080 (1996)

[26] T. Kato, K. Saeki, H. Nishide, T. Yamada, development of CNG fueled engine with lean burn for small size commercial van, JSAE Rev. **22**, 365–368 (2000)

[27] U. Kesgin, Effect of turbocharging system on the performance of a natural gas engine, Energ. Convers. Manage. **46**, 11–32 (2005)

[28] U. Kesgin, Efficiency improvement and NOx emission reduction potentials of two-stage turbocharged Miller cycle for stationary natural gas engines, Int. J. Energ. Res. **29**, 189–216 (2005)

[29] M. Altosole, G. Benvenuto, U. Campora, F. Silvestro, G. Terlizzi, Efficiency improvement of a natural gas marine engine using a hybrid turbocharger, Energies **11**, 1924 (2018)

[30] K. Luo, Y. Huang, Z. Han, Y. Li, Y. Shi, W. Liu, C. Tang, Low-speed performance compensation of a turbocharged natural gas engine by intake strategy optimization, Fuel **324**, 124748 (2022)

[31] S. Rousseau, B. Lemoult, M. Tazerout, Combustion characterization of natural gas in a lean burn spark-ignition engine, P. I. Mech. Eng. D-J. Aut. **213**, 481–489 (1999)

[32] L. Ben, N. Raud-Ducros, R. Truquet, G. Charnay, Influence of air/fuel ratio on cyclic variation and exhaust emission in natural gas SI engine, SAE Technical Paper No. 1999 – 01–2901

[33] U. Kesgin, Effect of turbocharging system on the performance of a natural gas engine, Energ. Convers. Manage. **46**, 11–32 (2005)
[34] Q. Tang, J. Fu, J. Liu, F. Zhou, X. Duan, Study of energy-saving potential of electronically controlled turbocharger for internal combustion engine exhaust gas energy recovery, ASME J. Eng. Gas Turb. Power **138** (2016)
[35] K.S. Hoyer, M. Sellnau, J. Sinnamon, H. Husted, Boost system development for gasoline direct-injection compression-ignition (GDCI), SAE Int. J. Engines **6**, 815–826 (2013)
[36] C. Chadwell, T. Alger, C. Roberts, S. Arnold, Boosting simulation of high efficiency alternative combustion mode engines, SAE Int. J. Engines **4**, 375–393 (2011)
[37] M. Özkan, D.B. Özkan, O. Özener, H. Yılmaz, Experimental study on energy and exergy analyses of a diesel engine performed with multiple injection strategies: effect of pre-injection timing, Appl. Therm. Eng. **53**, 21–30 (2013)
[38] Q. Tang, J. Fu, J. Liu, B. Boulet, L. Tan, Z. Zhao, Comparison and analysis of the effects of various improved turbocharging approaches on gasoline engine transient performances, Appl. Therm. Eng. **93**, 797–812 (2016)
[39] V. De Bellis, S. Marelli, F. Bozza, M. Capobianco, 1D simulation and experimental analysis of a turbocharger turbine for automotive engines under steady and unsteady flow conditions, Energy Procedia **45**, 909–918 (2014)
[40] F. Payri, J. Benajes, M. Reyes, Modelling of supercharger turbines in internal-combustion engines, Int. J. Mech. Sci. **38**, 853–869 (1996)
[41] A.V. Passar, D.V. Tymoshenko, E.V. Faleeva, Application of a new design and calculation technology for improving the blading section of the engine with turbine supercharger, in: Defect and Diffusion Forum, Khabarovsk, Russia, 2019
[42] M. Yang, Y. Gu, K. Deng, Z. Yang, S. Liu, Influence of altitude on two-stage turbocharging system in a heavy-duty diesel engine based on analysis of available flow energy, Appl. Therm. Eng. **129**, 12–21 (2018)
[43] J. Wahlström, L. Eriksson, Modelling diesel engines with a variable-geometry turbocharger and exhaust gas recirculation by optimization of model parameters for capturing non-linear system dynamics, P. I. Mech. Eng. D-J. Aut. **225**, 960–986 (2011)
[44] J.B. Heywood, Internal combustion engine fundamentals, 1ª Edição. Estados Unidos **25**, 1117–1128 (1998)
[45] GB/T 23341.2-2009, Turbochargers—Part 2:Test methods [S]

Cite this article as: F. Zhou, Z. Meng, X. Xiao, J. Fu, K. Yuan, Z. Cui, J. Yu, J. Liu, Pre-matching study of the natural gas engine turbocharging system based on the coupling of experiments and numerical simulation, Mechanics & Industry **25**, 2 (2024)